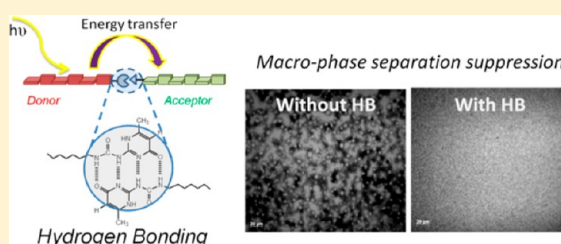


Supramolecular Conjugated Block Copolymers

Yen-Hao Lin,[†] Seth B. Darling,^{‡,||} Maxim P. Nikiforov,[‡] Joseph Strzalka,[§] and Rafael Verduzco^{*,†}[†]Department of Chemical and Biomolecular Engineering, MS 362, Rice University, 6100 Main Street, Houston, Texas 77005, United States[‡]Center for Nanoscale Materials, Argonne National Laboratory, 9700 South Cass Avenue, Argonne, Illinois 60439, United States[§]X-ray Science Division, Advanced Photon Source, Argonne National Laboratory, Argonne, Illinois 60439, United States^{||}Institute for Molecular Engineering, The University of Chicago, 5747 South Ellis Avenue, Chicago, Illinois 60637, United States

S Supporting Information

ABSTRACT: While the performance of polymer–polymer bulk heterojunction organic photovoltaics (OPVs) is poor compared with polymer–fullerene OPVs, reducing or eliminating micrometer-scale phase separation in all-polymer OPVs may dramatically improve performance. Herein, we demonstrate that 2-ureido-4[1H]-pyrimidinone (UPy) quadruple hydrogen bonding interactions can be used to prevent micrometer-scale phase separation at temperatures and processing conditions typically used to prepare bulk heterojunction OPVs. UPy-terminated polymers are synthesized by coupling hydroxyl or primary amine terminated polymers to a reactive isocyanate–UPy group in a one-step reaction. Polymer blend films are subsequently prepared by solution blending, casting onto a surface, and thermal and/or solvent annealing. Film microstructure including the presence of phase-separated domains and polymer crystallinity is analyzed by optical microscopy, atomic force microscopy (AFM), and grazing-incidence wide-angle X-ray scattering (GIWAXS). In contrast to unmodified polymer blends, blends of UPy-terminated polymers do not exhibit micrometer-scale phase separation after extended thermal annealing. AFM reveals the presence of crystalline nanofibers and, in some cases, 100–300 nm phase-separated domains in UPy-mediated polymer blends. Fluorescence measurements indicate that UPy modification increases fluorescence quenching in solutions of donor and acceptor polymers, due to hydrogen-bonding associations which reduce the average distance for energy and/or electron transfer. These results show that UPy-mediated interactions can suppress micrometer-scale phase separation in bulk heterojunction polymer blends at temperatures and processing conditions typically used to prepare bulk-heterojunction OPVs. As a result, UPy functionalization may be a powerful route for improving the performance of all-polymer OPVs.



■ INTRODUCTION

The nanoscale structure of the active layer plays a key role in determining the efficiency of photon-to-electricity conversion in bulk heterojunction (BHJ) organic photovoltaics (OPVs), which are typically comprised of a blend of p-type (hole-conductive) and n-type (electron-conductive) organic semiconductors. While some degree of phase separation is desired for creating continuous charge transport pathways, micrometer-scale phase separated domains are unfavorable due to reduced interfacial area and decreased charge separation efficiencies.^{1–4} This presents significant challenges for all-polymer OPVs, which are made up of a blend of a p-type and n-type conjugated polymers; micrometer-scale phase separation is commonly observed due to the reduced entropy of mixing for polymer blends.^{5–8} While the best performance in all-polymer OPVs (~2%)^{9–13} is significantly lower compared with state-of-the-art polymer–fullerene BHJs, reducing or eliminating large-scale phase separation in all-polymer OPVs may dramatically improve performance. Advantages of all-polymer OPVs over polymer–fullerene OPVs include a typically higher V_{oc} , broader absorbance, and tunability of the absorption profile due to the presence of two polymeric semiconductors in the active layer.

All-conjugated block copolymers with p- and n-type blocks represent a promising approach to improving the performance of all-polymer OPVs. Phase separation can be avoided and block copolymer self-assembly may lead to ideal structures for charge dissociation and transport.^{14,15} However, studies on donor–acceptor all-conjugated block copolymers are limited, due in large part to synthetic challenges,^{16–28} and noncovalent interactions may provide a more accessible approach to construct materials that exhibit the desirable properties of all-conjugated block copolymers.^{29–31} Noncovalent associations such as hydrogen bonds,^{32,33} ionic bonds,^{34,35} and metal–ligand coordination³⁶ give rise to persistent intermolecular associations between monomeric or polymeric units resulting in supramolecular polymers. These associations potentially provide a straightforward method to reduce phase separation in all-polymer OPVs, resulting in improved performance and model materials for understanding the structure of conjugated polymer blends.

Received: April 24, 2012

Revised: July 15, 2012

Published: July 31, 2012

The ureidopyrimidone (UPy) group forms self-complementary quadrupole hydrogen bonding interactions with high dimerization constants (up to 10^7 M^{-1} in nonpolar solvents such as chloroform).^{37–39} Supramolecular polymers based on UPy interactions have been widely studied, and recent work with coil-like (nonconjugated) polymers has shown that hydrogen bonding interactions can reduce phase separation in polymer blends.^{32,38,40–42} The UPy group is also effective in mediating the microstructure and optoelectronic properties of organic semiconductors. For example, UPy hydrogen bonding interactions can enhance energy transfer between electron donor and acceptor molecules⁴³ and improve interfacial contact and ionic conductivity when incorporated in the polymer electrolyte of a dye-sensitized solar cell.⁴⁴ Also, white-light emitting diodes have been demonstrated using UPy-mediated supramolecular interactions between semiconductive oligomers.⁴⁵

Herein, we present a study of the structure, optoelectronic properties, and crystallization of blends of polymers modified with UPy groups. Conjugated and nonconjugated polymers are functionalized with UPy in a one-step coupling reaction and solution blended to form supramolecular conjugated block copolymers. A practical advantage of UPy interactions compared with all-conjugated block copolymers is a greatly simplified synthetic route and straightforward preparation through solution blending. The structure of blend films is analyzed under a variety of annealing conditions using a combination of polarized optical microscopy (POM), atomic force microscopy (AFM), and grazing-incidence wide-angle X-ray scattering (GIWAXS). We find that UPy quadruple hydrogen bonding interactions can prevent micrometer-scale phase separation in polymer blend thin films and increase fluorescence quenching in solution due to a reduced average distance between donor and acceptor polymers.

EXPERIMENTAL SECTION

Materials. Methyl isocytosine (MIC) was purchased from Sigma-Aldrich and dried under vacuum at 100°C overnight before use. Styrene (purchased from Sigma-Aldrich) was purified by passing through an Al_2O_3 column. Poly(ethylene glycol) methyl ether (PEG-OH, 5000 g/mol) was purchased from Sigma-Aldrich. 2-(6-Isocyanatohexylaminocarbonylamino)-6-methyl-4[1H]-pyrimidinone (UPy-isocyanate),³⁸ 2,5-dibromo-3-hexylthiophene,⁴⁶ 9',9'-dioctylfluorene-2',7'-diboronic pinacol ester, and 7'-bromo-9',9'-dioctylfluorene-2'-yl-4,4,5,5-tetramethyl[1,3,2]dioxaborolane⁴⁷ were synthesized as previously described. Tetrahydrofuran (THF) and chloroform (CHCl_3) were dried over molecular sieves (4 Å). All other reagents were purchased from Sigma-Aldrich and used as received. Silicon wafers were purchased from El-Cat, washed by sonication in DI water and isopropyl alcohol, and dried under a stream of compressed air before use.

Aniline-End Functionalized Poly(3-hexylthiophene), P3HT-NH₂. P3HT-NH₂ was prepared using a procedure adapted from a previous report.³⁵ In a 50 mL flask purged with nitrogen gas, 2,5-dibromo-3-hexylthiophene (1.9 g, 5.82 mmol) was dissolved in anhydrous THF (5 mL), and the solution was stirred under nitrogen at 0°C for 15 min. A solution of isopropyl magnesium chloride and LiCl (1.3 M) in THF (4.48 mL, 5.82 mmol) was added, and the mixture was stirred for 2 h. Then, 25 mL of THF was then added before adding Ni(dppp)Cl_2 (105.15 mg, 0.194 mmol), and the mixture was stirred for 15 min. The reaction was quenched by adding a 1 M THF solution of 3-[bis(trimethylsilyl)amino] phenylmagnesium chloride (6 mL, 6 mmol) and stirring for 15 min. Then 5 M HCl (8 mL, 40 mmol) was added, and the solution was stirred for another 15 min. The final mixture was collected by precipitation in cold methanol and water and then by washing with CHCl_3 in a Soxhlet

apparatus. The CHCl_3 solution was stirred with 2 M Na_2CO_3 solution to neutralize the aniline end group. The resulting product was precipitated in cold methanol and dried at 50°C under vacuum. Yield: 0.86 g (88%). M_w (GPC): 4986 g/mol, $\text{dn/dc} = 0.250$, polydispersity (PDI) = 1.17, Degree of polymerization (DP) (NMR) = 30. ^1H NMR (400 MHz, CDCl_3), δ (ppm): 6.95 (30H; Aryl-H), 3.75 (2H; NH_2), 2.82 (60H; $\text{C}-\text{CH}_2-\text{C}_5\text{H}_{11}$), 1.70 (60H; $\text{CH}_2-\text{CH}_2-\text{C}_4\text{H}_9$), 1.35 (180H; $\text{CH}_2-\text{C}_3\text{H}_6-\text{CH}_3$), 0.92 (90H; CH_2-CH_3).

Hydroxyl-End Functionalized Poly(9,9-dioctylfluorenyl-2,7-diyl), PFO-OH. 7'-Bromo-9',9'-dioctylfluorene-2'-yl-4,4,5,5-tetramethyl[1,3,2]dioxaborolane (1 g, 1.68 mmol), 4-(Hydroxymethyl)phenylboronic acid pinacol ester (19.6 mg, 0.08 mmol), Tetrakis(triphenylphosphine)palladium(0) (75 mg, 0.065 mmol), and Aliquat 336 (3 drops) were added to a Schlenk tube loaded with nitrogen-purged toluene (25 mL) and 2 M Na_2CO_3 aqueous solution (10 mL). The reaction was stirred in 90°C oil bath for 1 day. 4-(Hydroxymethyl)phenylboronic acid pinacol ester (157 mg, 0.67 mmol) was added to the reaction tube and the solution was stirred for 1 day at 90°C . Bromobenzene (large excess) was added to the reaction and stirred for an additional day before collecting the product by precipitation in methanol. The polymer was subsequently washed with copious amounts of methanol and acetone and dried under vacuum. Yield: 520 mg (84%). M_w (GPC): 5860 g/mol, $\text{dn/dc} = 0.234$, PDI = 1.31, DP (NMR) = 13. ^1H NMR (400 MHz, CDCl_3), δ (ppm): 7.5–7.8 (87H; -Ph), 4.78 (2H; Ar- CH_2-OH), 2.1 (52H; $\text{CH}_2-\text{C}_7\text{H}_{15}$), 1.13 (260H; $\text{CH}_2-\text{C}_5\text{H}_{10}-\text{CH}_3$), 0.80 (78H; $\text{C}_7\text{H}_{14}-\text{CH}_3$).

Hydroxyl-End Functionalized Poly(9,9-dioctylfluorenyl-2,7-diyl)-co-(2,3,5-benzothiadiazole), PFBT-OH. 9',9'-Dioctylfluorene-2',7'-diboronic pinacol ester (812 mg, 1.265 mmol), 4,7-dibromobenzo[1,2,5]thiadiazole (370 mg, 1.265 mmol), 4-(hydroxymethyl)phenylboronic acid pinacol ester (14.8 mg, 0.063 mmol), tetrakis(triphenylphosphine)palladium(0) (75 mg, 0.065 mmol), and Aliquat 336 (3 drops) were added to a Schlenk tube loaded with nitrogen-purged toluene (25 mL) and 2 M Na_2CO_3 aqueous solution (10 mL). The reaction was stirred in 90°C oil bath for 1 day. 4-(Hydroxymethyl)phenylboronic acid pinacol ester (118 mg) was added to the reaction tube, and the solution was stirred for 1 day at 90°C . 4-bromobenzyl alcohol (283 mg) was added to the reaction, and the solution was stirred for 1 day at 90°C . The polymer was recovered by precipitation in methanol, washed with copious amounts of methanol and acetone, and dried under vacuum. Yield: 620 mg (81%). M_w (GPC): 15320 g/mol, $\text{dn/dc} = 0.263$, PDI = 1.37, DP (NMR) = 22. ^1H NMR (400 MHz, CDCl_3), δ (ppm): 7.3–8.2 (184H; -Ph), 4.78 (4H; Ar- CH_2-OH), 2.1 (88H; $\text{CH}_2-\text{C}_7\text{H}_{15}$), 1.13 (440H; $\text{CH}_2-\text{C}_5\text{H}_{10}-\text{CH}_3$), 0.80 (132H; $\text{C}_7\text{H}_{14}-\text{CH}_3$).

Hydroxyl-End Functionalized Polystyrene, PS-OH. Bromine-terminated polystyrene (PS-Br) was first synthesized by mixing styrene (12 g, 115.2 mmol), Cu^+Br (200 mg, 1.38 mmol), PMDETA (0.29 mL), and ethyl α -bromoisobutyrate (0.127 mL, 0.86 mmol) under nitrogen and reacting at 65°C . The polystyrene product was precipitated in cold methanol and dried at 50°C under vacuum. Next, PS-Br ($M_w \sim 10\,000$, 1.6 g, 0.16 mmol), ethanolamine (0.5 mL), and Et_3N (1 mL) were dissolved in DMF (25 mL) and stirred at room temperature overnight. The product was precipitated in cold methanol and dried at 50°C under vacuum. Yield: 5 g (50%). M_w (GPC): 9851, $\text{dn/dc} = 0.173$, PDI = 1.04. DP (NMR) = 97. ^1H NMR (400 MHz, CDCl_3), δ (ppm): 6.45–7.08 (490H; -Ph), 3.42 (2H; O- CH_2-CH_3), 3.36 (2H; - CH_2-OH), 3.10 (1H; NH-CH-Ph), 2.10 (2H; NH- $\text{CH}_2-\text{CH}-\text{OH}$), 1.84 (194H; $\text{CH}_2-\text{CH}-\text{Ph}$), 1.42 (97H; $\text{CH}_2-\text{CH}-\text{Ph}$), 0.99(6H; C-(CH_3)₂), 0.83 (3H; O- CH_2-CH_3).

General Procedure for the Preparation of UPy-End Functionalized Polymers. All UPy-end terminated polymers were prepared using the same procedure, except where indicated otherwise. In a representative procedure, P3HT-NH₂ (300 mg, 0.075 mmol), UPy-isocyanate (65.9 mg, 0.225 mmol), and 3 drops of dibutyltin dilaurate (DBDTL) were dissolved in dry CHCl_3 and stirred at 50°C for 24 h. Silica gel (240 mesh, 10 mg) was subsequently added, and the solution was stirred at 60°C for 24 h. The crude product was precipitated in cold methanol (PEG-UPy was precipitated from cold

diethyl ether), loaded into a Soxhlet apparatus, and washed with CHCl_3 to collect the final product, which was concentrated under reduced pressure and dried under vacuum. Recovered yield: 261 mg, 87%. ^1H NMR data for each polymer is provided in the text below and in the Supporting Information.

UPy-Functionalized Polystyrene (PS-UPy). Yield (recovered): 90%. ^1H NMR (500 MHz, CDCl_3), δ (ppm): 13.15 (1H; -NH), 11.88 (1H; -NH), 10.18 (1H; -NH), 5.82 (1H; -CH), 6.45–7.08 (490H; -Ph), 3.42 (2H; O-CH₂-CH₃), 3.21 (2H; -CH₂-O-isocyanate-UPy), 3.10 (1H; NH-CH-Ph), 2.10 (2H; NH-CH₂-CH-OH), 1.84 (194H; CH₂-CH-Ph), 1.42 (97H; CH₂-CH-Ph), 0.99 (6H; C-(CH₃)₂), 0.83 (3H; O-CH₂-CH₃).

UPy-Functionalized Poly(ethylene glycol) (PEG-UPy). Yield (recovered): 92%. ^1H NMR (400 MHz, CDCl_3), δ (ppm): 13.15 (1H; -NH), 11.88 (1H; -NH), 10.18 (1H; -NH), 5.82 (1H; -CH), 3.4–3.8 (452H; O-CH₂-CH₂-O-), 3.35 (3H; O-CH₃), 3.21 (4H; NH-CH₂), 2.20 (3H; NH-C-CH₃); 1.63 (4H; -CH₂-CH₂-), 1.35 (4H; NH-CH₂-CH₂-).

UPy-Functionalized Poly(3-hexyl thiophene) (P3HT-UPy). Yield (recovered): 87%. ^1H NMR (500 MHz, CDCl_3), δ (ppm): 13.15 (1H; -NH), 11.88 (1H; -NH), 10.18 (1H; -NH), 5.82 (1H; -CH), 6.95 (30H; Aryl-H), 3.75 (1H; NH-UPy), 2.82 (60H; C-CH₂-C₅H₁₁), 1.70 (60H; CH₂-CH₂-C₄H₉), 1.35 (180H; CH₂-C₃H₆-CH₃), 0.92 (90H; CH₂-CH₃).

UPy-Functionalized Poly(9,9-dioctyl fluorene) (PFO-UPy). Yield (recovered): 85%. ^1H NMR (500 MHz, CDCl_3), δ (ppm): 13.15 (1H; -NH), 11.88 (1H; -NH), 10.18 (1H; -NH), 5.82 (1H; -CH), 7.5–7.8 (87H; -Ph), 5.12 (2H; Ar-CH₂-O-UPy), 2.1 (52H; CH₂-C₇H₁₅), 1.13 (260H; CH₂-C₅H₁₀-CH₃), 0.80 (78H; C₇H₁₄-CH₃).

UPy-Functionalized Poly(9,9-dioctyl fluorene-*alt*-benzothiadiazole) (PFBT-UPy). Yield (recovered): 87%. ^1H NMR (500 MHz, CDCl_3), δ (ppm): 13.15 (2H; -NH), 11.88 (2H; -NH), 10.18 (2H; -NH), 5.82 (2H; -CH), 7.3–8.2 (184H; -Ph), 5.12 (4H; Ar-CH₂-OH), 2.1 (88H; CH₂-C₇H₁₅), 1.13 (440H; CH₂-C₅H₁₀-CH₃), 0.80 (132H; C₇H₁₄-CH₃).

Instrumentation. Size Exclusion Chromatography (SEC). Molecular weights and polydispersities were obtained by SEC using an Agilent 1200 module equipped with three PSS SDV columns in series (100, 1000, and 10000 Å pore sizes), an Agilent variable wavelength UV/vis detector, a Wyatt Technology HELEOS II multiangle laser light scattering (MALLS) detector ($\lambda = 658$ nm), and a Wyatt Technology Optilab reX RI detector. This system enables SEC with simultaneous refractive index (SEC-RI), UV/vis (SEC-UV/vis), and MALLS detection. THF was used as the mobile phase at a flow rate of 1 mL/min at 40 °C.

Nuclear Magnetic Resonance (NMR). ^1H NMR spectroscopy was performed on Bruker 400 MHz spectrometers for all OH- and NH₂-terminated polymers and Varian 500 MHz for all UPy-terminated polymers. Samples were placed in 5 mm o.d. tubes with sample concentrations of about 5 mg/mL. Solvents contain 0.05% TMS as an internal standard.

Polarizing Optical Microscopy. Optical microscopy images of polymer blend films were acquired using an Axioplan 2 imaging microscope in reflective mode. Films were prepared by spin-casting 6 mg/mL solutions onto a silicon wafer cleaned by sonication in DI water and isopropyl alcohol. Images were processed using Axio Vision version 4.8.

Fourier Transform Infrared (FTIR). FTIR analysis was carried out using a Thermo-Nicolet Nexus 670 instrument operated via the OMNIC program. Samples were prepared by depositing approximately 1 mg of bulk polymer on the sample holder.

Atomic Force Microscopy (AFM). AFM analysis was performed using a Veeco Multimode 8 with NanoScope V Controller (instruments located at the Center for Nanoscale Materials at Argonne National Laboratory and the Center for Functional Nanomaterials at Brookhaven National Laboratory) and a Multimode with Nanoscope IIIA controller at Rice University. Sample topography was recorded using Tapping and PeakForce modes. Second order flattening has been used for compensation of sample tilt and enhancement of image contrast. Sample films were prepared by spin-casting a 6 mg/mL

solution onto a silicon substrate and thermally annealing on a temperature controlled hot plate.

Ultraviolet–visible (UV–vis) absorbance and Luminescence spectrometer. UV–vis absorbance measurements were carried out with a Varian Cary 50 spectrophotometer with scan range of 190–1100 nm, and fluorescence quenching measurements were carried out on a Jobin-Yvon Horiba NanoLog spectrofluorimeter. Samples for fluorescence measurements were prepared by stirring 1 mg/mL solutions in CHCl_3 overnight before diluting to a concentration of approximately 1 $\mu\text{g/mL}$ P3HT or P3HT-UPy. The actual P3HT or P3HT-UPy concentration in the sample was estimated by measuring the optical density at 510 nm, and normalized fluorescence data were obtained by scaling the raw fluorescence measurement by the actual concentration of P3HT or P3HT-UPy in solution.

Grazing Incidence Wide-Angle X-ray Scattering (GIWAXS).

Grazing incidence wide-angle X-ray scattering measurements were carried out on Sector 8-ID-E at Advanced Photon Source, Argonne National Laboratory.⁴⁸ Beamline 8-ID-E operates at an energy of 7.35 keV and images were collected from a Pilatus 1MF camera (Dectris), with two exposures for different vertical position of the detector. After flatfield correction for detector nonuniformity, the images are combined to fill in the gaps for rows at the borders between modules, leaving dark only the columns of inactive pixels at the center. Using the GIXSGUI package⁴⁹ for Matlab (Mathworks), data are corrected for X-ray polarization, detector sensitivity and geometrical solid-angle. The beam size is 200 μm (h) \times 20 μm (v). Sample detector distance is 204 mm. Sample measurement and thermal annealing were carried out under vacuum which is in the range of $2\text{--}3 \times 10^{-6}$ bar, with the sample stage interfaced with a Lakeshore 340 unit.

RESULTS AND DISCUSSION

Synthesis of UPy-Functionalized Polymers. Supramolecular block polymers can be prepared by blending UPy-functionalized homopolymers. UPy is a self-complementary group, and as a result the blend is expected to consist of A–A, A–B, and B–B associations (Figure 1b). To investigate phase-separation, crystallinity, and optoelectronic properties of supramolecular block copolymers, both conjugated and non-conjugated UPy-functionalized polymers were prepared. Specifically, three conjugated polymers—poly(3-hexylthiophene) (P3HT), poly(9,9-dioctyl fluorene) (PFO), and poly(9,9-dioctyl fluorene-*alt*-benzothiadiazole) (PFBT)—and two coil-like polymers—poly(ethylene glycol) (PEG) and polystyrene (PS)—were studied. P3HT is a widely studied p-type polymer in bulk-heterojunction OPVs. PFO has been utilized in both OPVs and OLEDs, and a variety of PFO copolymers exhibit broad absorbance, low bandgap, and, in some cases, electron transport.⁵⁰ PFBT has measurable electron mobility,⁴² and bulk heterojunction blends of PFBT and P3HT exhibit a 0.13% power conversion efficiency.⁵¹ PS and PEG are chosen as model coil-like polymers for their ease of preparation and relevance to a number of block copolymer systems.

As shown schematically in Figure 1a, UPy-terminated polymers can be prepared through a one-step coupling reaction involving hydroxyl or primary amine-functionalized polymers and isocyanate-functionalized UPy.³⁸ As evidenced by ^1H NMR and FTIR, this enables the preparation of UPy-terminated polymers with a high degree of functionalization due to the reactivity of isocyanate groups toward primary hydroxyl and amine functionalities (Figures 2 and 3). All UPy-functionalized polymers prepared exhibited four distinct NMR peaks corresponding to the terminal UPy group - δ (ppm) = 13.15 (-NH), 11.88 (-NH), 10.18 (-NH), and 5.82 (-CH) (Figure 2a and S5–S9). PS, PFO, and PFBT also exhibit a clear shift in the ^1H NMR peak corresponding to CH₂ adjacent to the terminal hydroxyl group (Figure 2). For PS-OH, the ^1H NMR peak

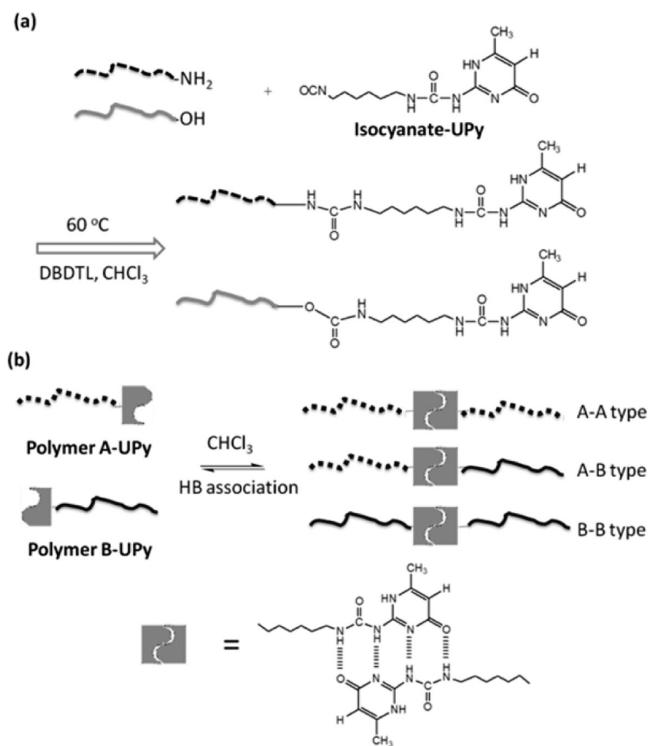


Figure 1. Schematic of (a) the synthetic scheme for preparation of UPy-terminated polymers and (b) quadruple hydrogen bonding (HB) associations between different UPy-terminated polymers to form supramolecular block copolymers.

corresponding to terminal CH_2 shifts from δ (ppm) = 3.36 to 3.21 after the coupling reaction (Figure 2b). In the case of PFO-OH and PFBT-OH (see Supporting Information, Figures S2 and S3), the terminal CH_2 ^1H NMR peak shifts from δ (ppm) = 4.78 to 5.12 (Figure 2c).

FTIR spectroscopy (Figure 3) provides further evidence for UPy functionalization of P3HT and PFO. MIC, a precursor to the UPy end group, exhibits a sharp primary amine ($-\text{NH}_2$) peak at 3330 cm^{-1} and a peak at 1655 cm^{-1} corresponding to the carbonyl group ($\text{C}=\text{O}$). After reaction with hexyl diisocyanate, the primary amine peak vanishes and a peak at 2282 cm^{-1} corresponding to free isocyanate ($\text{N}=\text{C}=\text{O}$) appears. A new peak near 3235 cm^{-1} corresponding to a secondary amine also appears, and split peaks at 1655 cm^{-1} reflect hydrogen bonding interactions between the carbonyl group and the secondary amine functionality. P3HT- NH_2 exhibits two weak signals at around 3400 and 3500 cm^{-1} , and after functionalization with UPy a broad peak at 3380 cm^{-1} appears, indicative of a secondary amine functional group. PFO-OH has a small peak at around 3450 cm^{-1} corresponding to the primary hydroxyl group, and the peak disappears after functionalization with UPy. FTIR was less reliable for analyzing end-group functionalization of PEG-OH, PS-OH, and PFBT-OH (see Supporting Information, Figure S10).

Phase Behavior of Polymer Blends in Thin Films. In order to test the effect of UPy associations on phase behavior, blend films were cast on a surface and analyzed by optical microscopy and AFM. Samples were thermally annealed near but below the highest crystallization temperatures (180 and $110\text{ }^\circ\text{C}$ for 5K P3HT and PFO, respectively) before analysis by POM. These annealing conditions were chosen because a clear difference was observed in the phase behavior of UPy and non-

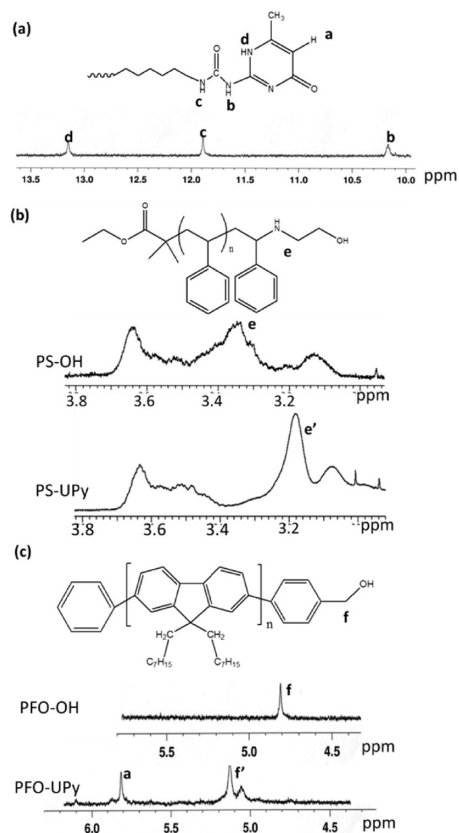


Figure 2. ^1H NMR data for (a) the UPy end group, (b) polystyrene before and after coupling to UPy, and (c) poly(9,9-dioctyl fluorene) before and after coupling to UPy.

UPy polymer blends. POM analysis shows that UPy-mediated hydrogen bonding interactions suppress micrometer-scale phase separation at these annealing conditions (Figure 4). For example, in the case of P3HT/PS blends mixed at a 50/50 ratio by mass, clear evidence for micrometer-scale phase separation is observed after annealing overnight at $160\text{ }^\circ\text{C}$ (Figure 4a). By contrast, no micrometer-scale phase separation is observed for P3HT-UPy/PS-UPy blend films (Figure 4b). Similar results are observed for PFO/PEG blend films annealed at $100\text{ }^\circ\text{C}$ (Figures 4c and 4d), P3HT/PEG blend films annealed at $160\text{ }^\circ\text{C}$ (see Supporting Information, Figure S11), and P3HT/PFO blend annealed at $160\text{ }^\circ\text{C}$ (Figures 4e and 4f). Results for PS/PFO blend films were inconclusive since no phase separation was observed for both PS/PFO and PS-UPy/PFO-UPy blends (Supporting Information, Figure S12). Altogether, these results indicate that UPy-functionalized conjugated polymer blends have a reduced tendency for micrometer-scale phase separation.

While a clear difference between UPy and non-UPy-terminated polymers was observed for the specific annealing conditions described above, higher temperature treatment conditions were tested to explore the limit of miscibility of UPy-terminated polymer blends. All blend films studied, including UPy polymer blends, showed micrometer-scale phase separation when solvent annealed at $170\text{ }^\circ\text{C}$ in the presence of dichlorobenzene (see Supporting Information, Figure S13) or when thermally annealed (without solvent present) at $190\text{ }^\circ\text{C}$ (higher than the crystalline temperature of the present P3HT sample) (see Supporting Information, Figure S14). On the other hand, no phase separation was observed by

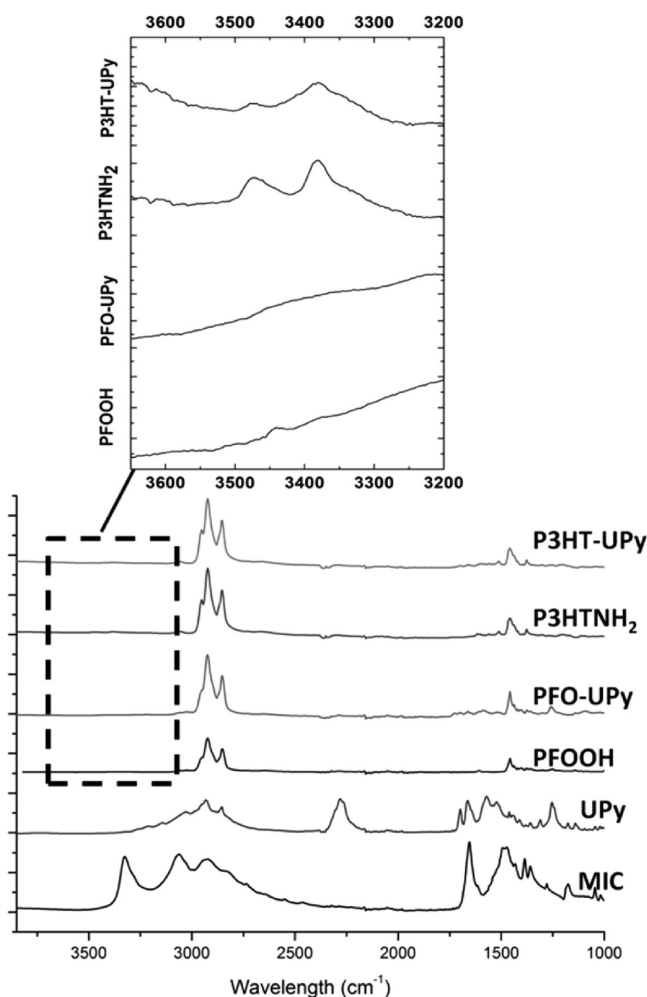


Figure 3. FTIR spectra for various end-functionalized polymers as well as the reactive UPy–isocyanate group (UPy) and methyl isocytosine (MIC).

POM after annealing overnight at 100 °C for any polymer blend (see Supporting Information, Figure S12, for an

example). These results indicate that thermal annealing at 190 °C or at 170 °C in the presence of dichlorobenzene is required to induce micrometer-scale phase separation in P3HT–UPy blends. By comparison, other studies on UPy-functionalized molecules have shown that associations are disrupted at a temperature of approximately 80 °C when solvent is present,^{52,53} and a report on star-shaped UPy end-functionalized polymers found associations persist only to temperatures as high as 130 °C.⁵⁴ A recent study on UPy-functionalized nonconjugated polymers reported micrometer-scale phase separation in polymer blend films thermally annealed at just 100 °C.³² Thus, the results in the present study indicate that blends consisting of one or more conjugated polymers can increase the temperature required for phase separation. This may be due to a combination of thermodynamic and kinetic effects, as discussed below.

GIWAXS measurements were carried out on pristine P3HT–UPy films, P3HT films, and P3HT blend films to investigate crystallization in UPy-modified polymers and polymer blends (Figures 5 and 6). In the case of P3HT–UPy, as-cast films show little or no crystallinity, but on heating to 80 °C characteristic P3HT-crystallite peaks appear and persist up to temperatures of 160 °C (Figure 5). The positions and intensity of crystalline peaks is qualitatively similar to those of P3HT films prepared similarly and measured at an elevated temperature (Figure 6a). Furthermore, thermally annealed (160 °C, 16 h) P3HT–UPy/PFO–UPy and P3HT–UPy/PS–UPy blend films exhibit similar crystalline peaks (Figure 6, parts b and c), but the intensity of the crystal peaks is significantly weaker for blend films compared with pristine P3HT films. These measurements indicate that crystallization is still present but reduced in UPy-modified polymer blend films.

AFM measurements were carried out to investigate the mesoscale structure of UPy polymer blend films.⁵⁵ AFM images show clear evidence for crystallization in pristine P3HT, pristine PFO, and their blend films with UPy-mediated interactions. For example, AFM topography images of P3HT–UPy/PS–UPy blend films reveals crystalline nanowires characteristic of P3HT with fiber dimensions approximately 10 nm in width and lengths up to 100 nm after 16 h of thermal

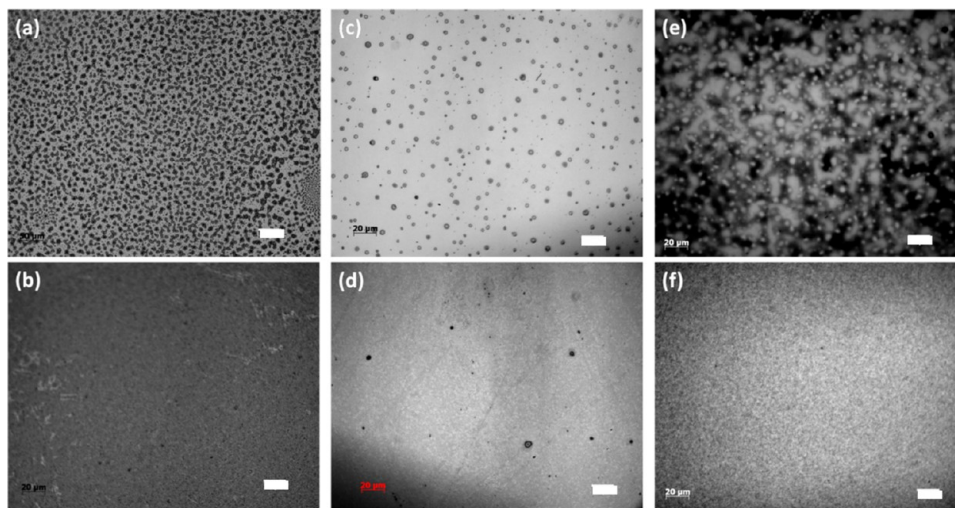


Figure 4. Optical microscopy images of thermally annealed polymer blends: (a) 50/50 wt % P3HT/PS, (b) 50/50 wt % P3HT–UPy/PS–UPy, (c) 50/50 wt % PFO/PEG, (d) 50/50 wt % PFO–UPy/PEG–UPy, (e) 50/50 wt % P3HT/PFO, and (f) 50/50 wt % P3HT–UPy/PFO–UPy. Scale bar: (a) 50 μ m, and (b–f) 20 μ m. Thermal annealing conditions: (a, b, e, and f) 160 °C, 16 h; (c and d) 100 °C, 16 h.

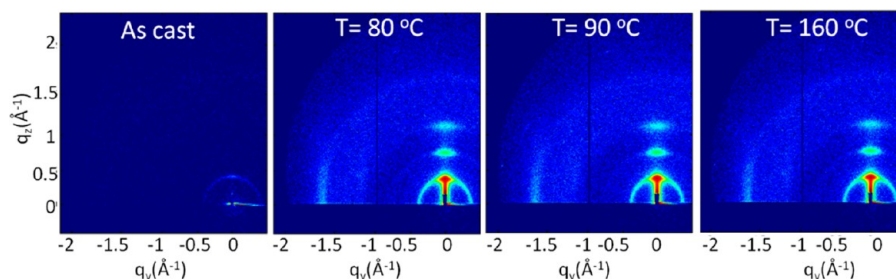


Figure 5. GIWAXS patterns of a P3HT–UPy thin films cast at room temperature and thermally annealed in situ. All samples were measured at an incident angle of 0.25° and 20 s exposure time, and all images have the same color scale.

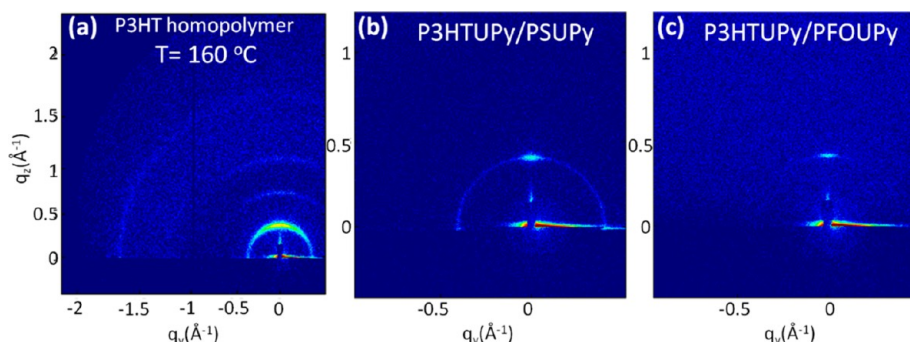


Figure 6. GIWAXS patterns of (a) P3HT homopolymer annealed in situ at 160°C , (b) P3HT–UPy/PS–UPy, and (c) P3HT–UPy/PFO–UPy measured at room temperature after thermal annealing for 16 h at 160°C . All samples were measured at an incident angle of 0.25° and 20 s exposure time, and all images have the same color scale.

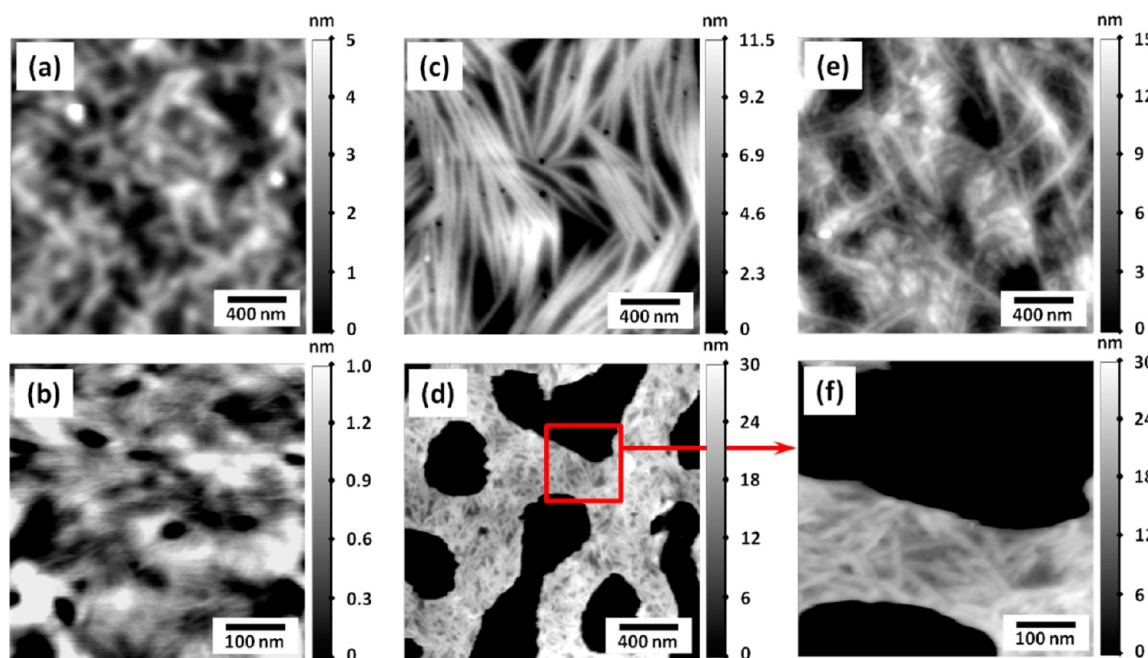


Figure 7. Atomic force microscopy height images of thermally annealed polymer films: (a) pristine P3HT–NH₂, (b) 50/50 wt % P3HT–UPy/PS–UPy, (c) PFO, (d) 50/50 wt % PFO–UPy/PEG–UPy, (f) 50/50 wt % PFO–UPy/PEG–UPy in smaller scale, and (e) 50/50 wt % P3HT–UPy/PFO–UPy. Thermal annealing conditions: (a, b, and e) 160°C , 16 h; (c, d, and f) 100°C , 16 h.

annealing at 160°C (Figure 7b). Pristine PFO films also exhibit crystalline fibers after thermal annealing at 100°C for 16 h (Figure 7c), with fiber dimensions of about 50 nm in width and lengths up to $1\ \mu\text{m}$. In the case of PFO–UPy/PEG–UPy annealed at 100°C for 16 h, both crystallization and submicrometer-scale phase separation are observed, with phase-separated domains roughly 300 nm in size (Figure

7d,e). Crystalline fibers are only present in the PFO-rich domains and have fiber dimensions approximately 20 nm in width and lengths up to 200 nm. Similar fibril structures with dimensions of about 30 nm in width and 700 nm in length were observed in P3HT–UPy/PFO–UPy blends annealed at 160°C for 16 h with no evidence of phase separation. Submicrometer phase separation was also observed in

P3HT-UPy/PEG-UPy and PFO-UPy/PS-UPy blends (Supporting Information, Figure S16). Furthermore, for P3HT-UPy/PFO-UPy and P3HT-UPy/PS-UPy, solvent annealing at room temperature for 4 days gives rise to nanoscale phase-separated domains with P3HT crystallinity (see Supporting Information, Figure S18).

Altogether, AFM and POM measurements of thermally annealed polymer blend films indicate that UPy-mediated interactions can suppress micrometer-scale phase separation in conjugated polymer blend films thermally annealed at temperatures up to 160 °C. The reduced tendency for micrometer-scale phase separation may be due to a combination of thermodynamic and kinetic effects. Previous work indicates that UPy-mediated hydrogen bonding interactions are weak above 100 °C,^{52,53} but crystallization in P3HT-UPy blends persists up to 180 °C and may lead to reduced chain mobility and slower kinetics for phase-separation. This is consistent with the GIWAXS data that show significant crystallinity present in P3HT-UPy at 160 °C and AFM images, which indicate that phase separation occurs at a reduced length scale in some UPy-terminated polymer blend films (e.g., PFO-UPy/PEG-UPy). On the other hand, UPy-modification may also affect the thermodynamics of polymer blends, resulting in a homogeneous phase for some UPy-polymer blends. This is supported by mean-field theories for supramolecular block copolymers that indicate complete miscibility under some conditions^{56,57} and may explain the absence of microphase segregated structures in UPy polymer blends.

Fluorescence Quenching in Conjugated Polymer Blends. Fluorescence measurements were carried out on P3HT/PFO and P3HT/PFBT solution blends to determine if UPy-mediated interactions between donor and acceptor polymers affect fluorescence quenching. UPy associations are expected to decrease the average distance between polymers compared with unmodified polymer blends, resulting in increased fluorescence quenching. PFBT has a more compatible LUMO level for energy transfer with P3HT and is therefore expected to exhibit more significant quenching compared with PFO.²⁸

Fluorescence quenching measurements were carried out by selectively exciting P3HT; this is accomplished by choosing an excitation wavelength greater than 510 nm, above which PFO and PFBT exhibit no absorbance (Figure 8a). The measurements therefore probe energy and/or electron transfer from P3HT to PFO or PFBT, and a quantitative comparison can be made by preparing solutions with approximately the same P3HT content (1–5 $\mu\text{g/mL}$) and normalizing fluorescence spectra by the overall P3HT concentration, estimated by the measured absorbance at 510 nm.

The fluorescence spectrum (see Supporting Information, Figure S17) of pure P3HT and P3HT-UPy solutions shows that the terminal UPy group by itself has a negligible impact on fluorescence quenching. Blends of unmodified polymers show lower fluorescence compared with that of pristine P3HT or P3HT-UPy, indicative of some energy or electron transfer from P3HT to PFO or PFBT, and as expected quenching is more significant for P3HT/PFBT solution blends due to better matching of LUMO energy levels (Figure 8b). Furthermore, for both P3HT/PFO and P3HT/PFBT, UPy-modified polymer blends exhibited lower fluorescence compared with that of non-UPy modified polymer blends. This indicates that UPy-associations increase fluorescence quenching due to decreased

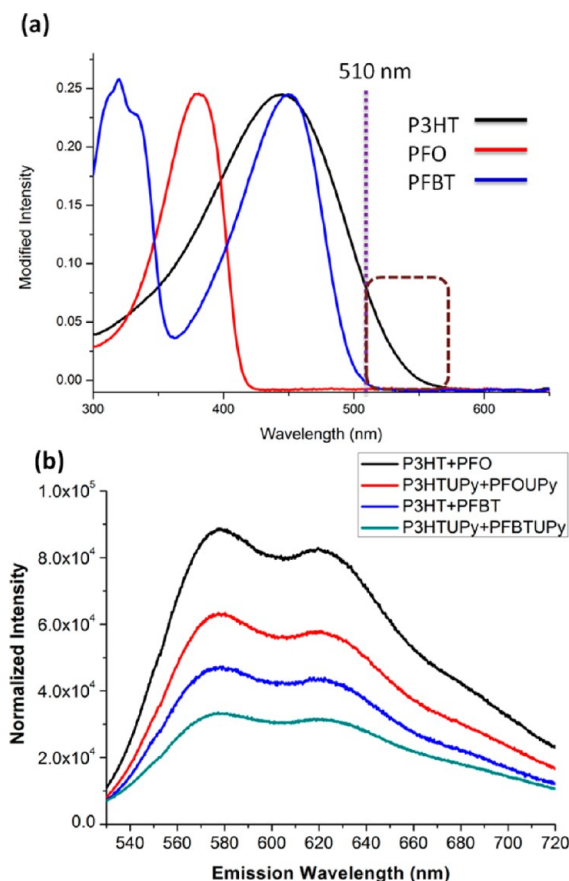


Figure 8. (a) UV-vis absorbance spectra of P3HT, PFO, and PFBT. The dotted line indicates the excitation wavelength used for fluorescence measurements; note that only P3HT exhibits significant absorbance at 510 nm. (b) Fluorescence spectra for conjugated polymer blends in solution under 525 nm excitation wavelength.

average distance between donor and acceptor polymers in solution.

CONCLUSION

A series of conjugated and nonconjugated UPy-terminated polymers were synthesized via a one-step reaction with UPy-isocyanate. A combination of AFM, POM, and GIWAXS shows that UPy-mediated quadruple hydrogen bonding interactions can prevent micrometer-scale phase separation in conjugated polymer blends. UPy modification increases fluorescence quenching in solutions of donor and acceptor polymers, due to hydrogen-bonding associations which reduce the average distance for energy and/or electron transfer. These results show that UPy-mediated interactions can suppress micrometer-scale phase separation in bulk heterojunction polymer blends at temperatures and processing conditions typically used to prepare bulk-heterojunction OPVs. As a result, UPy functionalization may be a promising route for improving the performance of all-polymer OPVs.

ASSOCIATED CONTENT

Supporting Information

¹H NMR spectra of polymers prepared, POM images of polymer blend films, AFM images of polymer blend films, fluorescence data, and GIWAXS data. This material is available free of charge via the Internet at <http://pubs.acs.org>.

■ AUTHOR INFORMATION

Corresponding Author

*E-mail: rafaelv@rice.edu.

Notes

The authors declare no competing financial interest.

■ ACKNOWLEDGMENTS

This work was carried out with support from the Welch Foundation for Chemical Research (Grant #C-1750), the Shell Center for Sustainability, and Louis and Peaches Owen. We gratefully acknowledge Tao Sun for assistance with the GIWAXS measurements. Use of the Center for Nanoscale Materials and Advanced Photon Source at Argonne National Laboratory was supported by the U.S. Department of Energy, Office of Science, Office of Basic Energy Sciences, under Contract No. DE-AC02-06CH11357. Research carried out in part at the Center for Functional Nanomaterials, Brookhaven National Laboratory, which is supported by the U.S. Department of Energy, Office of Basic Energy Sciences, under Contract No. DE-AC02-98CH10886.

■ REFERENCES

- (1) Gunes, S.; Neugebauer, H.; Sariciftci, N. S. *Chem. Rev.* **2007**, *107*, 1324–1338.
- (2) Thompson, B. C.; Fréchet, J. M. J. *Angew. Chem., Int. Ed.* **2008**, *47*, 58–77.
- (3) Hoppe, H.; Sariciftci, N. S. *J. Mater. Res.* **2004**, *19*, 1924–1945.
- (4) Peet, J.; Heeger, A. J.; Bazan, G. C. *Acc. Chem. Res.* **2009**, *42*, 1700–1708.
- (5) Veenstra, S. C.; Loos, J.; Kroon, J. M. *Prog. Photovolt.: Res. Appl.* **2007**, *15*, 727–740.
- (6) McNeill, C. R.; Greenham, N. C. *Adv. Mater.* **2009**, *21*, 3840–3850.
- (7) Kim, J.-S.; Ho, P. K. H.; Murphy, C. E.; Friend, R. H. *Macromolecules* **2004**, *37*, 2861–2871.
- (8) McNeill, C. R.; Watts, B.; Thomsen, L.; Ade, H.; Greenham, N. C.; Dastoor, P. C. *Macromolecules* **2007**, *40*, 3263–3270.
- (9) McNeill, C. R.; Abrusci, A.; Zaumseil, J.; Wilson, R.; McKiernan, M. J.; Burroughes, J. H.; Halls, J. J. M.; Greenham, N. C.; Friend, R. H. *Appl. Phys. Lett.* **2007**, *90*, 193506–3.
- (10) Kietzke, T.; Hörhold, H.-H.; Neher, D. *Chem. Mater.* **2005**, *17*, 6532–6537.
- (11) Koetse, M. M.; Sweelssen, J.; Hoekerd, K. T.; Schoo, H. F. M.; Veenstra, S. C.; Kroon, J. M.; Yang, X.; Loos, J. *Appl. Phys. Lett.* **2006**, *88*, 083504.
- (12) Granstrom, M.; Petritsch, K.; Arias, A. C.; Lux, A.; Andersson, M. R.; Friend, R. H. *Nature* **1998**, *395*, 257–260.
- (13) Holcombe, T. W.; Woo, C. H.; Kavulak, D. F. J.; Thompson, B. C.; Fréchet, J. M. J. *J. Am. Chem. Soc.* **2009**, *131*, 14160–14161.
- (14) Segalman, R. A.; McCulloch, B.; Kirmayer, S.; Urban, J. J. *Macromolecules* **2009**, *42*, 9205–9216.
- (15) Darling, S. B. *Energy Environ. Sci.* **2009**, *2*, 1266–1273.
- (16) Botiz, I.; Schaller, R. D.; Verduzco, R.; Darling, S. B. *J. Phys. Chem. C* **2011**, *115*, 9260–9266.
- (17) Mulherin, R. C.; Jung, S.; Huettner, S.; Johnson, K.; Kohn, P.; Sommer, M.; Allard, S.; Scherf, U.; Greenham, N. C. *Nano Lett.* **2011**, *11*, 4846–4851.
- (18) Sommer, M.; Komber, H.; Huettner, S.; Mulherin, R.; Kohn, P.; Greenham, N. C.; Huck, W. T. S. *Macromolecules* **2012**, *45*, 4142–4151.
- (19) Woody, K. B.; Leever, B. J.; Durstock, M. F.; Collard, D. M. *Macromolecules* **2011**, *44*, 4690–4698.
- (20) Wu, S.; Bu, L.; Huang, L.; Yu, X.; Han, Y.; Geng, Y.; Wang, F. *Polymer* **2009**, *50*, 6245–6251.
- (21) Lai, Y.-C.; Ohshimizu, K.; Takahashi, A.; Hsu, J.-C.; Higashihara, T.; Ueda, M.; Chen, W.-C. *J. Polym. Sci., Part A: Polym. Chem.* **2011**, *49*, 2577–2587.
- (22) Scherf, U.; Gutacker, A.; Koenen, N. *Acc. Chem. Res.* **2008**, *41*, 1086–1097.
- (23) Ouhib, F.; Khoukh, A.; Ledeuil, J.-B.; Martinez, H.; Desbrières, J.; Dagron-Lartigau, C. *Macromolecules* **2008**, *41*, 9736–9743.
- (24) Ohshimizu, K.; Takahashi, A.; Higashihara, T.; Ueda, M. *J. Polym. Sci., Part A: Polym. Chem.* **2011**, *49*, 2709–2714.
- (25) Sun, S.-S.; Zhang, C.; Ledbetter, A.; Choi, S.; Seo, K.; Carl, E.; Bonner, J.; Drees, M.; Sariciftci, N. S. *Appl. Phys. Lett.* **2007**, *90*, 043117.
- (26) Chen, X. L.; Jenekhe, S. A. *Macromolecules* **1996**, *29*, 6189–6192.
- (27) Xiao, X.; Fu, Y.; Sun, M.; Li, L.; Bo, Z. *J. Polym. Sci., Part A: Polym. Chem.* **2007**, *45*, 2410–2424.
- (28) Verduzco, R.; Botiz, I.; Pickel, D. L.; Kilbey, S. M.; Hong, K.; Dimasi, E.; Darling, S. B. *Macromolecules* **2011**, *44*, 530–539.
- (29) Fox, J. D.; Rowan, S. J. *Macromolecules* **2009**, *42*, 6823–6835.
- (30) Rehm, T.; Schmuck, C. *Chem. Commun.* **2008**, 801–813.
- (31) Yang, S. K.; Ambade, A. V.; Weck, M. *Chem. Soc. Rev.* **2011**, *40*, 129–137.
- (32) Feldman, K. E.; Kade, M. J.; de Greef, T. F. A.; Meijer, E. W.; Kramer, E. J.; Hawker, C. J. *Macromolecules* **2008**, *41*, 4694–4700.
- (33) Dankers, P. Y. W.; Zhang, Z.; Wisse, E.; Grijsma, D. W.; Sijbesma, R. P.; Feijen, J.; Meijer, E. W. *Macromolecules* **2006**, *39*, 8763–8771.
- (34) Huh, J.; Park, H. J.; Kim, K. H.; Park, C.; Jo, W. H. *Adv. Mater.* **2006**, *18*, 624–629.
- (35) Takahashi, A.; Rho, Y.; Higashihara, T.; Ahn, B.; Ree, M.; Ueda, M. *Macromolecules* **2010**, *43*, 4843–4852.
- (36) Lohmeijer, B. G. G.; Schubert, U. S. *Angew. Chem., Int. Ed.* **2002**, *41*, 3825–3829.
- (37) Shokrollahi, P.; Mirzadeh, H.; Huck, W. T. S.; Scherman, O. A. *Polymer* **2010**, *51*, 6303–6312.
- (38) Folmer, B. J. B.; Sijbesma, R. P.; Versteegen, R. M.; van der Rijt, J. A. J.; Meijer, E. W. *Adv. Mater.* **2000**, *12*, 874–878.
- (39) Beijer, F. H.; Sijbesma, R. P.; Kooijman, H.; Spek, A. L.; Meijer, E. W. *J. Am. Chem. Soc.* **1998**, *120*, 6761–6769.
- (40) Lee, K. J.; Lee, D. K.; Kim, Y. W.; Kim, J. H. *Eur. Polym. J.* **2007**, *43*, 4460–4465.
- (41) Keizer, H. M.; Gonzalez, J. J.; Segura, M.; Prados, P.; Sijbesma, R. P.; Meijer, E. W.; de Mendoza, J. *Chem.—Eur. J.* **2005**, *11*, 4602–4608.
- (42) Wrue, M. H.; McUmber, A. C.; Anthamatten, M. *Macromolecules* **2009**, *42*, 9255–9262.
- (43) Wang, S. M.; Yu, M. L.; Ding, J.; Tung, C. H.; Wu, L. Z. *J. Phys. Chem. A* **2008**, *112*, 3865–3869.
- (44) Kim, Y. J.; Kim, J. H.; Kang, M. S.; Lee, M. J.; Won, J.; Lee, J. C.; Kang, Y. S. *Adv. Mater.* **2004**, *16*, 1753–1757.
- (45) Abbel, R.; Grenier, C.; Pouderoijen, M. J.; Stouwdam, J. W.; Leclere, P.; Sijbesma, R. P.; Meijer, E. W.; Schenning, A. J. *Am. Chem. Soc.* **2009**, *131*, 833–843.
- (46) Han, Y.-K. L.; Y-J; Huang, P.-C. *J. Electrochem. Soc.* **2009**, *156*, k37–k43.
- (47) Zhang, X.; Tian, H.; Liu, Q.; Wang, L.; Geng, Y.; Wang, F. *J. Org. Chem.* **2006**, *71*, 4332–4335.
- (48) Jiang, Z.; Li, X. F.; Strzalka, J.; Sprung, M.; Sun, T.; Sandy, A. R.; Narayanan, S.; Lee, D. R.; Wang, J. *J. Synchrotron Radiat.* **2012**, *19*, 627–636.
- (49) Jiang, Z., *GIXSGUI is available for download*: <http://www.aps.anl.gov/Sectors/Sector8/Operations/GIXSGUI.html>.
- (50) Herguth, P.; Jiang, X.; Liu, M. S.; Jen, A. K. Y. *Macromolecules* **2002**, *35*, 6094–6100.
- (51) Kim, Y.; Cook, S.; Choulis, S. A.; Nelson, J.; Durrant, J. R.; Bradley, D. D. C. *Chem. Mater.* **2004**, *16*, 4812–4818.
- (52) Yamauchi, K.; Lizotte, J. R.; Long, T. E. *Macromolecules* **2003**, *36*, 1083–1088.

- (53) Yamauchi, K.; Lizotte, J. R.; Hercules, D. M.; Vergne, M. J.; Long, T. E. *J. Am. Chem. Soc.* **2002**, *124*, 8599–8604.
- (54) Mather, B. D.; Elkins, C. L.; Beyer, F. L.; Long, T. E. *Macromol. Rapid Commun.* **2007**, *28*, 1601–1606.
- (55) Ramanathan, M.; Darling, S. B. *Prog. Polym. Sci.* **2011**, *36*, 793–812.
- (56) Anthamatten, M. J. *Polym. Sci., Part B: Polym. Phys.* **2007**, *45*, 3285–3299.
- (57) Feng, E. H.; Lee, W. B.; Fredrickson, G. H. *Macromolecules* **2007**, *40*, 693–702.